GEONICS LIMITED
1745 Meyerside Dr. Unit 8 Mississauga, Ontario Canada L5T 1C6

Tel: (905) 670-9580
Fax: (905) 670-9204
E-mail: geonics@geonics.com
URL: http://www.geonics.com

Technical Note TN-28

OPTIMAL DETECTION OF TDEM ANOMALIES UNDER CONDUCTIVE OVERBURDEN

J.D. McNeill

July, 1995

TECHNICAL NOTE TN-28

Optimal Detection of TDEM Anomalies Under Conductive Overburden

Introduction

Smith and Pridmore (1989) give an excellent overview of the problems associated with various geophysical techniques, including TDEM, in those areas of Australia which are covered with conductive overburden. Asten (1992) suggests computing and stripping the theoretical response of an equivalent layered conductive overburden model from field data in order to improve deep target detectability and interpretability: however, he deals with large fixed transmitter loop TDEM surveys. Dentith et al (1994) have presented a very useful compendium of the response of a variety of mineral deposits in Western Australia, where the problem of conductive overburden is often of major concern with various geophysical techniques. Perusal of these references (following a visit to Australia which involved extensive discussions with the geophysical staff of Western Mining Corporation) has led to some observations which might be of use in planning and executing coincident loop/in-loop TDEM surveys under conditions of conductive overburden.

Smith and Pridmore state in their introduction that, "The ancient land surface over much of Australia is characterized by depths of oxidation and weathering of up to 100 m. Alluvium in the form of transported silts, clays, and saline evaporite deposits is found in paleo-drainage systems. Laterite profiles have been developed over both alluvium and oxidized bedrock. Clays and saline groundwater give electrical resistivities in the range 0.3 ohm-metres to 100 ohm-

metres; overburden conductances in the range 0-100 siemens".

"In some cases, weathering (hydration) of magnetite produces a non-magnetic species of iron oxide in the weathered zone. In other cases the magnetic character is preserved. During the process of lateritization, a magnetic species of iron oxide, maghemite, is developed in the pisolite zone. Maghemite typically displays variable remanence, susceptibility and super-paramagnetic (SPM) behaviour. Pisolites may be concentrated by fluvial processes in buried paleo-channels".

These features are illustrated in Fig. 1 (taken from Smith and Pridmore). Although these authors state that the range of overburden conductance can extend to 100 siemens they also state that the Elura base metal deposit in N.S.W. "is an excellent example of a well developed arid weathering profile. A typical electrical section would be a thin (less than 10 m) resistive layer of say 50 to 240 Ωm overlying a conductive weathered layer of 10 to 30 Ωm extending to a depth of approximately 100 m. Below the weathered layer, fresh rock may have resistivities of several thousand Ωm in the absence of mineralization". From these observations we see that the overburden conductance

$$S=\sigma h=\frac{h}{\rho} \qquad (1)$$

where σ and ρ are the overburden conductivity and resistivity respectively, and h is the overburden thickness, apparently varies typically from 3 to 9 siemens.

Furthermore, examination of the large number of TDEM case-histories given in Dentith et al (1994), using calculations to be described below, shows that, when the effects of conductive overburden are evident, the overburden conductances are relatively uniformly distributed over the range from 1 to 10 siemens. The fact that overburden conductances often seem to be less than 10 siemens will allow us to use the horizontal thin sheet approximation to understand some of the effects of conductive overburden.

This technical note is divided into two sections. In the first section we will explore the nature of the response from a conductive overburden by examining the general response from a two-layered earth consisting of an electrically thick conductive overburden overlying a resistive bedrock. We will learn under what conditions the response from this geoelectric section (which has three variables, vis overburden thickness and resistivity and bedrock resistivity) can be approximated by that from an electrically thin horizontal sheet (with only one variable, sheet conductance). Such simplification makes it easier to calculate both the response from the overburden and consequent modification of response from the underlying orebody.

Note that it will be assumed that overburden and orebody are not in electrical contact. Such an assumption can lead to serious errors in the case of large loop transmitters, where galvanic current response can be significant, but is less serious for the coincident/in-loop configurations considered in this note, where galvanic current response is minimized.

In the second section we will consider various ways in which we can improve survey procedures

and data interpretation techniques to enhance the detectability of targets situated beneath conductive overburden. In this section we will not necessarily assume that the overburden is electrically thin.

Specifically, in part A we will discuss:

(1) the TDEM response from a conductive overburden, using both the full theory and the horizontal thin sheet approximation

(2) the effects of conductive overburden on the time behaviour of the target response and on target detectability.

and in part B:

(4) the various factors that determine the overall signal-to-noise ratio in TDEM surveys in regions of conductive overburden.

(5) various ways in which to improve target detection in the presence of conductive overburden, and finally

(6) various ways in which to strip overburden effects to enhance target recognition.

It should be noted that much of the material in this technical note has been derived from Kaufman and Keller (1985) with some additional material from McNeill et al (1984).

Part A. TDEM Response from Conductive Overburden

Consider the geometry shown in Fig. 2a in which a large circular TDEM transmitter of radius r is situated on a two-layered earth of upper layer thickness h and resistivity ρ_1, overlying a

basement of resistivity ρ_2, where ρ_2 is much greater than ρ_1. The receiver, geometrically small compared with r and h, has area $1m^2$ and is located at the centre of the transmitter loop, which is driven with a step function current $I(t)$.

As is well known, immediately after the transmitter current is reduced to zero, currents flow in the vicinity of the transmitter loop, distributed so as to maintain the magnetic field everywhere within the earth at the value that existed before transmitter turn-off. Because of finite resistivity ρ_1 of the overburden, the currents decay with time due to eddy current losses and their time-varying magnetic field generates current flow deeper in the overburden. At early times the currents are largely confined to the overburden and the resultant decaying magnetic field sensed by the receiver coil will be that from a homogeneous half-space of resistivity ρ_1. As time progresses the currents diffuse to greater depth in the overburden until they reach the resistive basement. Since $\rho_2 >> \rho_1$ there will be negligible current flow in the basement, and from this time onwards the currents essentially flow in the overburden as a ring of expanding radius and decreasing current density.

The time rate of change of the magnetic field measured by the receiver, $\dot{B}_z(t)$, is plotted in Fig. 2b for the case where the transmitter current I=10 amps, and h=100 m, ρ_1=20 Ωm, and ρ_2=1,000 Ωm (values typical of a conductive overburden). It is seen that the shape of the curve is very bland, that the initial amplitude is extremely large and, that, at late times the time decay is extremely rapid. Indeed the curve of $\dot{B}_z$ falls by 8 orders of magnitude in a time range of 2½ orders of magnitude, covering a very large dynamic range.

Many readers will be familiar with the techniques developed in Russia (Kaufman and Keller, 1983) for facilitating the interpretation of TDEM geoelectric soundings. Basically the data of $\dot{B}_z(t)$ shown in Fig. 2b are transformed into a curve of late-stage apparent resistivity ρ_τ, which is plotted as a function of τ, the time domain equivalent of skin depth, divided by h, the upper layer thickness.

The transformation from t to τ is given by

$$\tau = \sqrt{2\pi\rho_1 t 10^7} \tag{2}$$

where t = time (sec)

and transformation of $\dot{B}_z(t)$ to ρ_τ is given by

$$\rho_\tau = \frac{\mu}{4\pi t}\left(\frac{2\mu M}{5t\dot{B}_z(t)}\right)^{2/3} \tag{3}$$

where $\mu = 4\pi \times 10^{-7}$ H/m,

M = transmitter dipole moment

= transmitter loop area x current I,

and $\dot{B}_z(t)$ = voltage out of the receiver coil (volts per m^2)

Use of this transformation is fully described in Kaufman and Keller (1983) and (more briefly) in McNeill (1980).

The transformed data of Fig. 2b shown in Fig. 2c, has a very different shape. The new curve

can be divided into three parts (1) a descending branch, where $\tau/h<5$, (2) a relatively flat region where $5<\tau/h<10$, and (3) an ascending branch where $\tau/h>10$. The descending branch, where τ/h is small, corresponds, under Australian conditions, to early times at which measurement of the time response is not normally made, and will not be discussed further. Instead we will focus our attention on the latter two parts of the curve.

We first note that, around the range $5<\tau/h<10$, $\rho_\tau/\rho_1 \approx 1$ and is not a function of τ/h. Since $\rho_\tau/\rho_1 = 1$, $\rho_\tau = \rho_1$, the actual resistivity of the upper layer.

Furthermore equations (2) and (3) can be easily manipulated to show that

$$\dot{B}_z(\tau) \propto \frac{1}{\left[\frac{\rho_\tau(\tau)}{\rho_1}\right]^{3/2}\left[\frac{\tau}{h}\right]^5} \tag{4}$$

and thus when $\rho_\tau(\tau)$ is not a function of τ/h, i.e. in the range $5<\tau/h<10$,

$$\dot{B}_z(\tau) \propto \frac{1}{\tau^5} \tag{5}$$

$$\text{or} \quad \dot{B}_z(t) \propto \frac{1}{t^{5/2}} \tag{6}$$

and we have the well known time dependence for the late stage response of a TDEM system located over a homogeneous half space. Clearly, within the range $\tau/h<10$, the currents are confined to the upper layer and have not yet sensed the resistive basement.

On the other hand, at large values of τ/h greater than 20 we see from Fig. 2c that ρ_a/ρ_1 is approximately proportional to $(\tau/h)^2$ and thus from equation (4)

$$\dot{B}_z(t) \propto \frac{1}{\left(\left(\frac{\tau}{h}\right)^2\right)^{3/2}\left(\frac{\tau}{h}\right)^5} \tag{7}$$

$$\text{or} \quad \dot{B}_z(\tau) \propto \frac{1}{\tau^8} \tag{8}$$

$$\text{and finally} \quad \dot{B}_z(t) \propto \frac{1}{t^4} \tag{9}$$

and we have the equally well known time dependence for the late-stage response of a conductive horizontal thin sheet. The range $10<\tau/h<20$ clearly indicates the transition range from upper layer response as a homogeneous half-space to upper layer response as a horizontal thin sheet.

Now equation (2) can be reworked to show that the time corresponding to a specified value of τ/h is given by

$$t = \frac{h^2\left(\frac{\tau}{h}\right)^2}{2\pi\rho_1 10^7} \tag{10}$$

so that, if ρ_1=20 Ωm and h=100 m, then for τ/h=8, t=0.5 msec, and for τ/h=30, t=7 msec.

Examination of Fig. 2b shows that indeed at 5×10^{-4} sec the response is decaying as $t^{-5/2}$, and at 7×10^{-3} sec as t^{-4}.

One further point should be noted. We have seen that, for a resistive basement, at $\tau/h>20$ the time response becomes that of a horizontal thin sheet. From equation (10) with $\tau/h=20$

$$t=\frac{400h^2}{2\pi\rho_1 10^7} \qquad (11)$$

and we observe that the onset of horizontal thin sheet (HTS) behaviour is more strongly influenced by h than ρ_1.

Now under the HTS condition it is well known (Kaufman and Keller, 1983, McNeill, 1980) that the late-stage expression for the time rate of change of the decaying magnetic field is given by

$$\dot{B}_z(t)=\frac{3M\mu^4S^3}{16\pi t^4} \qquad (12)$$

where M = transmitter dipole moment

and $S = h/\rho_1$

= sheet conductance (siemens)

Equation (12) was used (as stated in the Introduction) to calculate S for the various data sets given in Dentith et al (1994).

It is evident from equation (12) that the amplitude of the late stage HTS behaviour is extremely sensitive to S, varying as S^3. Thus we will not be surprised to see large excursions in $\dot{B}_z$ as we traverse a survey area. The conductance S is equal to h/ρ_1, so these variations can be caused either by changes in overburden resistivity or bedrock topography.

Up to this point we have shown that, for a resistive basement and for $\tau/h>20$, the layered earth response can be satisfactorily approximated by that of a horizontal thin sheet. The effect from two other parameters, r/h and ρ_2/ρ_1, must now be examined. Fig. 2d shows a complete suite of curves for various ρ_2/ρ_1 with $r/h=0.5$. Fig. 2e shows a similar suite for $r/h=1.0$. As we would expect the only difference between the two sets of curves occurs at early times where $\tau/h<8$. In general, in the Australian environment, measurement of the time response typically commences at times of the order of 0.5 msec, at which, for the usual values of ρ_1 and h (20Ωm and 100 m, for example), $\tau/h>7$ and the influence of r/h on the curve shape can be ignored.

As to the effect of ρ_2/ρ_1 we will see later that, in order to strip off the overburden response, we will be interested in the range of τ/h less than 80 (at greater values of τ/h all responses have disappeared). We note from either Fig. 2d or 2e that, for the larger values of ρ_2/ρ_1 which are of interest to us (the evidence is that the host rock usually presents a conductivity contrast of at least 20) and within the range $20<\tau/h<80$ the only significant effect of reducing ρ_2/ρ_1 is to reduce the slope of the late state response, which can still generally be approximated by a straight line. Thus the effect of reducing the bedrock resistivity contrast from infinity will be to slightly decrease the decay rate from t^{-4}.

In summary we see that, within the range $20<\tau/h<80$ and over the range of ρ_2/ρ_1 of interest, to us, the layered earth response can be satisfactorily approximated by the horizontal thin sheet response given in equation (12), and we will use the HTS approximation to determine some of the effects of the conductive overburden. Later on, we will wish to strip off the effects of conductive overburden from the orebody response. For that purpose we will want to work over the larger range $8<\tau/h<80$ and we will also want to include the effect of finite ρ_2, so will use the more accurate responses shown in Fig. 2d or 2e. Even so, it is the simple behaviour of the thick conductive overburden response over the range of τ/h from 8 to 80 (corresponding to typical time response in the Australian environment from 0.5 to 50 msec) that will often allow us to separate out target response from conductive overburden response.

To illustrate the appearance of conductive overburden response Fig. 3 shows profiles of Sirotem data (coincident 200 m loops) kindly supplied by Western Mining Corporation. The data, in μV/amp and plotted using linear scales, show the large dynamic range occupied by the measured $\dot{B}_z$. Fig. 4, which shows the same data plotted on a log scale, illustrates that for all but the earliest times the time decay exponent is essentially the same at all survey stations; it is the amplitude (proportional to S^3) which is varying down the survey line. Finally Fig. 5 shows a detailed plot of the decay at station 8050 near the centre of the line. The decay, rapid at times greater than 1-2 msec, approaches t^4 at late times, and the calculated conductance S at late time is 4.4 siemens. Such data, which resembles much data taken in regions of conductive overburden in Australia, justifies our contention that analysis based on the horizontal thin sheet approximation will often be useful.

Affects of Conductive Overburden on Target Detection

It is well known (Kaufman and Keller, 1985) that, at the late stage, the eddy current response from bounded conductive targets obeys the approximate relationship

$$\dot{B}_T(t) \propto \frac{1}{\tau} e^{-t/\tau} \tag{13}$$

where, in this section, τ refers to the late stage time constant of a confined target (in conformity with North American usage) whereas in the previous section τ (as defined in equation (2)) referred to the time-domain equivalent of the half-space skin-depth (in conformity with Russian usage).

On the other hand the response from the HTS is given by equation (12) as

$$\dot{B}_{HTS} \propto \frac{S^3}{t^4} \tag{14}$$

In general there is relatively little coupling between the two responses and we can simply add them together to get the total response. Thus, a measure of the geological signal-to-noise ratio is given by the ratio of these quantities.

$$SNR = \frac{\dot{B}_T}{\dot{B}_{HTS}} \propto \frac{\frac{1}{\tau} e^{-t/\tau}}{\frac{S^3}{t^4}} = \left(\frac{\tau}{S}\right)^3 \left(\frac{t}{\tau}\right)^4 e^{-t/\tau} \tag{15}$$

Taking the time derivative of this equation and setting it equal to zero to obtain maximum ***SNR*** shows that maximum ***SNR*** occurs at $t=4\tau$, regardless of S. This is a surprisingly long time, at which time the target amplitude itself is very small ($e^{-4} = 1.83 \times 10^{-2}$).

Substituting $t = 4\tau$ in equation (15) shows that the maximum SNR is proportional to

$$SNR_{Max} \propto \left(\frac{\tau}{S}\right)^3 \tag{16}$$

For fixed τ, the SNR_{Max} decreases as S^3, which is the main reason for difficulties encountered in exploration in regions of conductive overburden. Conversely, for fixed S the SNR_{Max} increases as τ^3 . Although the initial target response decreases as $1/\tau$, the fact that the response extends further out in time more than compensates for the decrease. Fig. 6 shows plots of the total response, $\dot{B}_T + \dot{B}_{HTS}$ for various values of τ, and Fig. 7 shows a plot of SNR as a function of t/τ. From Fig. 6 we observe the strong effect that increasing τ has on target detectability. From Fig. 7 we see that, to obtain the best target response relative to overburden response, we must measure the total response from about $t=2\frac{1}{2}\tau$ to $t=6\tau$. Measurement at earlier or later times will add little to our ability to expose the target. Thus, assuming that good targets exhibit τ's in the range from 1-3 msec we must be able to make high quality measurements out to 10-20 msec. High quality means that the measurements must not be contaminated by environmental noise (spherics, power line noise, etc.) which requires, in turn, that we use a sufficiently large transmitter dipole moment to overcome these noise sources.

To summarize, the effects of conductive overburden are to greatly reduce the target/overburden signal-to-noise ratio, to make only the larger τ targets detectable, and to force us to make measurements at very late times in order to detect them.

Affects of Conductive Overburden on Target Response Time Behaviour

Having ascertained that the TDEM response from conductive overburden in the Australian environment can often be approximated by horizontal thin sheet (HTS) response, it is a simple matter to calculate approximately the effect of the overburden on the target response. The most significant of these effects is distortion of the "drive" emf in the target, i.e. of the emf which causes the target vortex currents to flow. Fig. 8a schematically shows the primary magnetic field that would exist in the vicinity of a target located in free space (the transmitter is assumed to have a linear ramp turn-off) and also the emf (which, by Faraday's law is proportional to the time derivative of the primary magnetic field) induced in the target, and which causes the vortex current to flow. If the target is located beneath a HTS the primary magnetic field beneath the overburden will exhibit a slower decay, as shown in Fig. 8b; the "drive" emf will be distorted as indicated in the figure. To evaluate the distortion in the drive emf we wish to calculate the time derivative of the magnetic field beneath the HTS at the target. This can easily be done using the image theory derived by Maxwell and described in Smythe (1968). This theory tells us that, for $t<0$, the subsurface magnetic field is that from the transmitter loop situated on the surface, but for $t>0$ it is that from the same transmitter, but with the transmitter now moving vertically upwards with constant velocity given by $v=1/(\mu S)$. Fig. 9a shows the vertical magnetic

field and Fig. 9b its time derivative (the "drive" emf) at a location 100m directly below a 100 m diameter transmitter loop situated on a 10 siemen HTS. We see that the drive has been smeared out over time of the order of a few msec.

It is important to note that, regardless of the distortion of $\dot{B}$ caused by the overburden, the total area under the drive emf curve

$$\int_o^\infty \frac{dB}{dt} dt = \int_o^\infty dB = B(\infty) - B(0) = B_p \qquad (17)$$

is always equal to B_p, the primary field that existed at the measurement point just before transmitter turn-off. This is important since, from linear circuit theory we know that if $R(t)$ is the response of a circuit (for instance our target) to a delta-function drive, the response to a time-varying drive defined as $D(t)=0$ for $t<0$, and $D(t)$ for $t>0$, is given at any time t by

$$R_o(t) = \int_o^t R(t-x)\ D(x)\ dx \qquad (18)$$

If the duration of the drive is still short enough so that the response varies slowly during the drive duration, which is centered at $t=t_0$

$$R_o(t) = R(t-t_o) \int_o^t D(x)\ dx\ =\ R(t-t_o)B_p \qquad (19)$$

As long as the duration of the drive emf is short compared to the response time of the target (i.e.

to τ) it is the area under the drive curve, i.e. B_p, which will determine the amplitude of the response, and distortions in the shape of $\dot{B}(t)$ will have no effect. There will be no reduction in target amplitude or shape at late time; the only effect will be a shift in time of the response of the order of the duration of the drive. Only the high frequency portion of the response, i.e. the early time behaviour, will be significantly altered by the conductive overburden.

What would happen if τ was not long compared with the duration of the drive? Again from equation (18), but this time assuming that R(t) varies quickly with time compared with D(t), we see that

$$R_o(t) \propto D(t) \int_o^t R(t-x)\, dx \qquad (20)$$

and rather than reflecting the target response, the new response is a modified version of the drive. Targets with response times of the order of the smeared drive or less, will exhibit a severely distorted response.

These effects are illustrated in Fig. 10. Fig. 10a shows the distorted drive emf resulting from a 10 siemen HTS, an exponential decay with time constant 5 msec, and results of convolving the drive with the exponent. As discussed above we observe that, for times greater than 2 msec, the convolution resembles the exponential except for a delay of about 1 msec. Fig. 10b shows similar curves, except that the target time constant is 0.5 msec (note the change of time scale). At time greater than 1 msec the convolved curve now resembles the drive emf.

For the scale of completeness one further point should be made. The drive emf at late time decays as t^{-4} (the magnetic field beneath the overburden is the same as that above it). This is much slower than an exponential decay at $t>>\tau$, and the result is that, at times late compared with the target time constant, the target vortex currents no longer decay exponentially, but follow the t^{-4} behaviour of the drive, as implied by equation (20). Since the receiver coil measures dB_z/dt the receiver output voltage arising from the target response at late times will decay as t^{-5}. This effect is shown in Fig. 10c, again for a 10 siemen overburden and for a target time constant of 3 msec. It is seen that the departure from exponential decay becomes significant at about 10 time constants, so it is unlikely that this phenomenon will be observed often.

In the same way that the conductive overburden distorted the free-space drive emf it will also distort the target response. In this case the "drive" emf arising from the target is typically many msec in duration, and $R(t)$ is the response of the overburden, shown above to be of the order of a msec. Thus equation (20) applies, which shows that the effect of the overburden on the target response will be minimal, mainly shifting it in time about 1 msec.

We conclude then, that for overburden conductance of the order of 10 siemens, the response from targets with τ greater than a few msec will be essentially unaffected except for a small time shift, but that the response from targets with τ = 1 msec or less will be seriously distorted. These times scale up and down directly with overburden conductance. Finally we note that, in regions of conductive overburden, effort spent in trying to keep the transmitter turn-off time very short will be wasted in view of the broadening effect of the overburden.

This concludes our discussion of the direct effects of conductive overburden on target response.

Part B. Techniques to Improve Target Detectability

Overall Survey Signal to Noise Ratio

In this section we will discuss the various components that affect overall survey signal-to-noise ratio and how to enhance the target response. We will assume TDEM survey configurations to be either coincident loop, or off-set loop, both of which are commonly used in Australia. Fig. 11 illustrates schematically the various noise components to be discussed.

(a) Electronic noise:

This is the basic noise limit caused by the coil and input circuitry of the receiver (not shown in the figure is the fact that it varies with gate time if the gate widths vary with gate time). In a well designed and well operated TDEM system electronic noise must never appear in the survey data since the receiver coil moment (product of receiver coil turns x area) should be large enough so that even in areas (or seasons) of very low atmospheric noise, the atmospheric noise always exceeds electronic noise. Seeing electronic noise means that the receiver coil moment is too small and implies that useful target signals will be lost in the receiver noise.

For example consider the following table which lists typical signal and noise levels in a late time gate (all values have been divided by the receiver coil turns area and are given as nV/m^2).

	Case 1	Case 2
	Rx moment too small	Rx moment correct
		(increased by 10)
Target response	5 nV/m^2	5 nV/m^2
Atmospheric noise	1 nV/m^2	1 nV/m^2
Electronic noise	5 nV/m^2	0.5 nV/m^2

In case 1 the signal to noise ratio, determined by electronic noise, is about unity, whereas in case 2 the receiver coil moment has been increased by 10 and the overall signal to noise ratio increased to 5.

Large moment receiver coils are relatively inexpensive compared with overall cost of equipment and cost of carrying out surveys, however their selection requires some care. Physically large single-turn coils are broad band but can exhibit sensitivity to SPM and IP effects if the receiver coil wire is located close to the transmitter wire, and, because of their large size, lateral spatial resolution is reduced. Smaller, multi-turn coils avoid these disadvantages, however, their bandwidth is necessarily much less, which can (sometimes seriously) distort the received signals at early times. A simple compromise is a multi-turn coil of diameter 10-20 m, which although somewhat difficult to handle, avoids the problems described above.

(b) Atmospheric noise:

This noise component really encompasses all types of electromagnetic interference picked up by

the receiver and includes "spherics", power line noise (including both 50/60 Hz magnetic fields and radio signals reradiated by the power lines), radio and radar signals directly received, etc. It can vary widely with location, season and time of day. Not shown in Fig. 11 is the fact that spectral distribution of this noise source will cause the noise level to vary with gate time if the gate widths vary with gate time. Learn from the instrument manufacturer the magnitude of the electronic noise (which can vary with receiver coil type) and ensure that the receiver coil moment is large enough so that atmospheric noise always prevails by at least a factor of two or three.

(c) Overburden noise:

This noise component has already been discussed above, where it was noted that optimum time to measure target response against overburden response is at $t \approx 4\tau$. It was further shown that the overburden generally obeyed the late stage behaviour at these times and was thus decaying as t^{-4}. This is an extraordinarily rapid decay and severely tests the dynamic range of any TDEM receiver. It is observed that in many TDEM surveys carried out in Australia most of the response is due to overburden, leaving very little dynamic range left for detection of targets. In frequency domain this would be equivalent to using a multi-frequency system with most of the frequencies chosen so high that they measured only overburden response.

The dynamic range is defined here as the ratio, at a fixed receiver gain setting, of the largest signal that can be handled without distortion by the receiver (usually set by the power supply voltages on the various amplifiers) to the minimum signal that can be accurately measured (set by the system noise). Obviously to optimally utilize the dynamic range so as to measure the

smallest possible signal, the receiver gain should be increased until the largest amplitude signals (or noise) are just about to clip. Two cases must be considered. In the first case the largest predetection signal is in fact noise (power line, etc.) which has large amplitude over much of the measurement time range: in this case not much can be done to improve the detection of small signals. In the second case, however, the noise levels are sufficiently low so that the maximum signal is the early stage of the transient response. In this case, to better measure the small signals at late time with a well designed TDEM receiver, it is quite acceptable to open system gain up to the extent that early gates saturate hard. In a good receiver the gate next to the saturated ones may contain measurement errors, but subsequent gates will be error free, and this procedure should always be carried out in order to maximize precious dynamic range. The only caveat is that the gain must not be increased to the point where atmospheric noise is saturating the system, since clipping this noise will cause serious system distortion.

We should be interested in both overburden response and target response. If atmospheric noise is not limiting the dynamic range, it is advisable to make two measurements, the first at low gain, to accurately measure overburden response, and the second at high gain to detect potential targets. To assist in making the decision as to what gains to use, it is mandatory to employ a receiver that allows the operator to plot the entire transient response in the field on an LCD screen so that he can identify the various components of the response. Spherics and power line noise are usually best observed on a linear plot, whereas the HTS response is usually easy to identify on a log/log plot of the decay.

(d) Enhancing target response:

This is, of course, the response that we wish to lift out of all the noise components. Our problem is generally that of detecting target response against large overburden response. As seen above, with typical overburden conductances of 3-10 siemens, and target time constants of the order of a few msec (targets with smaller time constants will be difficult to characterize due to the distorted nature of the drive emf, as described above), we will have optimum signal/overburden noise at about four time constants. We must ensure that the system is carefully optimized for measurements in the 10-20 msec range, which means in part that we must use large transmitter currents since, as we shall see below, we will wish to keep the physical area of the transmitter loop reasonably small compared with the depth of exploration. This presents no great problem in Australia since the terrain is usually reasonably flat and free of vegetation, and the transmitter power supply (batteries or generator) can be permanently installed in the back of a vehicle. Effective currents of 60-100 amps (using multiple transmitter loop turns if necessary) are highly desirable to keep the target plus overburden response well out of the environmental noise at 10-20 msec.

What about the actual size of the transmitter loop? It is not generally realized that a large loop can be an ineffective way of energizing moderate sized targets at moderate depths, whereas it is always very effective at energizing overburden response. The reason for this is simple. Consider a square transmitter loop of side length $2a$ carrying a current I. The vertical magnetic field from such a loop at depth z is given by

$$Hz_l = \frac{I\,(2a)^2}{2\pi(z^2+2a^2)^{1/2}\,(z^2+a^2)} \tag{21}$$

whereas the field from a dipole of the same moment, also at depth z, is

$$Hz_d = \frac{I(2a)^2}{2\pi z^3} \tag{22}$$

The ratio $\boldsymbol{R}$ of these two quantities, is given by

$$R = \frac{1}{(1+2\frac{a^2}{z^2})^{1/2}\,(1+\frac{a^2}{z^2})} \tag{23}$$

Within the HTS approximation the overburden response from either source (of equal moments) will be the same, so this ratio is a measure of the ability to energize a small target relative to the overburden; it is shown in Fig. 12. It is evident that, if a/z = 1, (i.e. a small target at depth 100 m, energized by a 200x200 m loop) the relative (with respect to the overburden) target excitation is one-third that which would result from a dipole transmitter. As the target gets larger the relative excitation increases, but it is always advisable to use as small a transmitter loop as possible. We must increase transmitter dipole moment by increasing current and/or the number of turns.

The same observation applies to the receiver coil, but here there are more advantages to using a small loop. First, as the size of the receiver coil increases it too becomes relatively less

efficient at picking up flux from the target compared with that from the overburden since the flux from the target increases relatively slowly with increasing loop size (a larger portion of the secondary field becomes parallel to the plane of the loop) whereas, in the late stage, the magnetic field from the overburden is essentially uniform at the receiver and increasing receiver area directly increases overburden response. The net result is that equation (23) also gives the ratio of flux from a small target to that from the overburden. Multiplying the two ratios together shows the inadvisability of using large loops.

Although these comments are made for small targets they apply to a certain extent to all but the largest targets, so small transmitter and receiver loops should be the rule. In the case of the receiver coil a physically small coil is easily achieved using multi-turn loops: the only expense will be reduced bandwidth (which smears out the response at early times) but it can be shown, using arguments similar to those used in our discussion of overburden effects on drive emf, that bandwidths of a few kHz will not be a problem at measurement times of 10-20 msec, and can also be easily taken into account in modelling.

Two other reasons for using a small receiver coil are SPM and IP, both of which are usually localized in the vicinity of the transmitter wire, from which the receiver coil should be well separated. It is often said in Australia that SPM is usually not a problem, however, the technique of plotting out the transient response as apparent resistivity (to be described below) is a very sensitive detector of SPM and suggests that it may be more of a problem than is generally thought.

A final advantage of using small loops is that spatial resolution is substantially improved, resulting in better target diagnostics and location. For example, Fig. 13 shows two different transmitter and receiver loop configurations for detecting both horizontal and vertical plate targets. The plate has strike length of 200 m and depth extent of 100 m. The horizontal plate is buried at a depth of 100 m, and the vertical plate to a depth of 100 m to the top. The transmitter current and number of turns on the receiver coil have been adjusted so as to give transmitter and receiver moments equivalent to 200 m x 200 m. Note the better resolution for the smaller coils; the improved signal/overburden response is 4.3 for the horizontal plate and 2.5 for the vertical plate, not negligible improvements. It should be noted that, when using a small receiver coil within the transmitter loop, the receiver coil should be reasonably centrally located (to within a few meters) since an offset can cause a small asymmetry in the response.

In much of TDEM survey data seen from Australia it appears that too small a transmitter dipole moment was employed. The evidence for this is that a typical set of data profiles (usually plotted with logarithmic ordinate) shows only overburden response on the early and intermediate channels, whilst the target responses just start to become interesting at the latest times, at which the signals are disappearing into atmospheric noise. Since, as we have seen, large loops are not the answer, we recommend use of a 100x100m transmitter loop, of 3 turns of #10 wire, driven by a 3kW transmitter (either battery or motor generator powered) probably permanently mounted in the back of a small vehicle. Such a system would deliver a current of 20 amps into the loop, multiplied by 3 turns to give effectively 60 amps, compared with the normal 4-5 amps. Such a loop, while heavier than the ones deployed now, could still be relatively easily laid out and

moved. At the same time the recommended receiver coil would be a flexible 14x14 m coil with 50 turns, to give a total turns-area of approximately 10,000 m^2. Such a loop would, of course, be centrally located in the transmitter loop.

Finally, for those who wish to take data with both central and offset receiver coils, two such flexible receiver coils should be deployed with a two channel receiver which allows data from each coil to be taken simultaneously to improve survey speed.

Improving Target Recognition

The question arises as to how best to identify and quantify a target against a background response of conductive overburden. The problem is simple when the target response rests on overburden response that is relatively uniform; in this case the spatial profiles of TDEM response will often themselves suffice. But a problem arises when the overburden response is continually varying, or worse, just varying over the target. How can we determine the local overburden response to enable us to separate target response from overburden?

A simple approach is simply to plot out, at every station, the total time decay on log/log scales and to look for deviations from the HTS response. However, as we have seen from Fig. 5 this approach has the disadvantage that it will be difficult to see small exponential responses superimposed on the HTS response, due to the very large dynamic range of the latter.

A second approach would be to multiply the data by t^4, which would partially solve the dynamic

range problem, but this presents another problem because in real life the basement resistivity is never infinite, and as we have seen the effect of this is, over a large range of time, to make the decay rate effectively t^x where x probably lies between 3 and 4 depending on the resistivity contrast between the overburden and the basement.

A third, and undoubtedly the best solution, is to convert the transient data to apparent resistivity using equation (3), and to plot the data as one would for a normal sounding. Such a plot, for various values of ρ_2/ρ_1 and ρ_1 = 10 Ωm, h = 100 m, is shown in Fig. 14, where it is seen that the data is nicely compressed and that the responses for different values of ρ_2/ρ_1 are still very simple. Such a presentation also has the significant advantage that, because of the enormously reduced dynamic range, any problems with the data are obvious, and appropriate steps can be taken to correct them. Another advantage is that, using standard sounding theory, this format is very convenient for calculating the three parameters of the two larger geoelectric model, vis ρ_1, h and ρ_2. Fig. 15a shows the data of Figs. 3-5 (specifically station 8050) replotted as apparent resistivity. The somewhat strange nature of the data at this station produces a peculiar curve which, however, makes much more sense when superimposed on a two-layer curve of the type shown in Fig. 14 as is done in Fig. 15b; analysis gives ρ_1 = 15 Ωm, h = 160 m, and $\rho_2 = 20\rho_1$ = 300 Ωm.

Referring again to Fig. 14, it should be noted that, since SPM response causes an abnormally large signal at late time (approximately t^{-1} decay) the apparent resistivity will be too small at late time, and the approximately linear response shown on this figure will be replaced by $\rho_a(t)$ which

saturates and then decreases with increasing time, readily observable on this type of plot.

Fig. 16 shows the results of adding an exponential signal of the form $(1/\tau)\ \exp(-t/\tau)$ to the layered earth response. Fig. 16a shows a typical overburden transient decay to which has been added the exponential response of τ=5 msec. Fig. 16b shows the data converted to apparent resistivity; the presence of the exponential anomaly is quite apparent. Identification of the exponential will be relatively easy since all overburden responses will look much the same as the one illustrated. Having estimated the overburden response from the total response on this plot, the interpreter simply notes the values of the estimated overburden resistivity for each time channel, converts this data back to transient voltages, and subtracts them from the total response to obtain the amplitude of the target response along the survey profiles.

For the reasons given above it is felt that conversion to apparent resistivity is the best approach for target identification. Fig. 17 shows actual survey data form the same survey as Fig. 15. When plotted on a log-log plot the anomaly is difficult to characterize, particularly if adjacent anomaly-free data was not available. However, when plotted as apparent resistivity in Fig. 17 the presence of the anomaly is obvious, even through significant survey noise. Furthermore the maximum anomaly occurs at about 20 msec; since t/τ=4 we conclude that $\tau \approx$5msec.

Summary

(1) It is apparent that, in the Australian environment, it is necessary to make measurements of the transient response out to times at least 4 times the target time constant, and thus out to 10-

20 msec, to optimize target signal to overburden response. At that time the target response is very small; the overburden response can often be approximated by a horizontal thin sheet.

(2) Use of large transmitter dipole will ensure that, at these late times, the measured signal is well above environmental noise. A large receiver coil dipole moment will ensure that the atmospheric noise is well above receiver noise.

(3) Physically small transmitter and receiver loops are more efficient at energizing target response and rejecting the effects of conductive overburden. The large transmitter dipole must be achieved by the use of large transmitter current (60-100 amps, achieved, if necessary, by using multiple turns). The large receiver dipole must be achieved by the use of a physically small multi-turn receiver coil so as to swamp receiver noise. Such a physically small receiver coil will also mitigate against IP and SPM effects. The latter are a particular problem since they often distort the received signal at the late times when it is most important to measure its amplitude correctly. Use of small loops will appreciably improve both target resolution and target response with respect to overburden response.

(4) In view of the substantial overburden response which imposes a great burden on the receiver dynamic range it is recommended that two measurements be made at each measurement station (a) a measurement at relatively early time to accurately obtain the overburden response, and (b) a measurement at late time with receiver gain increased so that, although the early gates will now be saturated with overburden response, the useful dynamic range will extend to latest

times where it is anticipated that the useful signal/overburden noise ratio will be maximized. It should be noted that in TDEM measurements it is almost always better to take a series of three measurements at shorter integration time rather than one long measurement at three times the integration time. The three short measurements are compared and, if one is noisy, it is discarded and the other two averaged for the final data set.

(5) To separate out target response from overburden response it is suggested that the data be plotted as late-stage apparent resistivity in the usual manner for geoelectric soundings. This technique (a) provides an excellent check on the data quality, exposing instrument problems as well as the presence of SPM and IP, (b) allows rapid determination of the overburden/bedrock electrical parameters and (c) greatly facilitates detection of targets against the overburden response.

Bibliography

Asten, M.W., 1992, "Interpretation of Ground TEM Data from Conductive Terrains." Exploration Geophysics, 23, 9-16.

Dentith, M.C., et al, 1994, "Geophysical Signatures of Western Australian Mineral Deposits". ASEG Special Publication No. 7.

Kaufman, A., and Keller, G.V., 1983, "Frequency and Transient Soundings". Elsevier, N.Y

Kaufman, A., and Keller, G.V., 1985, Inductive Mining Prospecting. Part 1: Theory. Elsevier, N.Y.

McNeill, J.D., 1980, "Applications of Transient Electromagnetic Techniques". Geonics Limited, Technical Note TN-7.

McNeill, J.D., Edwards, R.N., and Levy, G.M., (1984), "Approximate calculations of the transient electromagnetic response from buried conductors in a conductive half-space": Geophysics, 49, 918-924.

Smith, R.J., and Pridmore, D.F., 1989, "Exploration in Weathered Terrains". Exploration Geophysics, 20, 411-434.

Smythe, W.R., 1968, "Static and Dynamic Electricity", McGraw Hill, N.Y.

Acknowledgements

The author would like to thank Peter Williams, Chief Geophysicist of Western Mining Corporation Limited, for inviting him to Australia in December, 1994. Many valuable and enjoyable discussions concerning the use of EM in the Australian environment took place at that time.

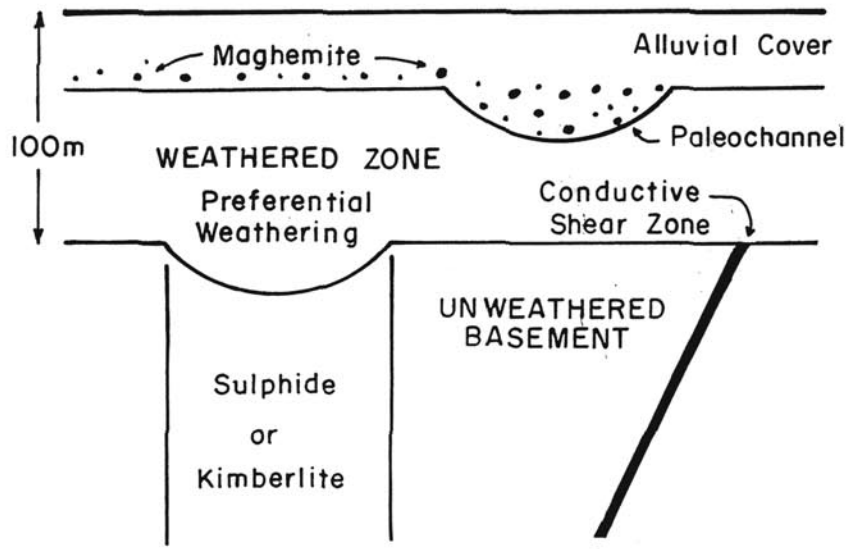

Fig. 1 *A schematic diagram illustrating a number of features of weathered terrain which affect the response of geophysical methods (from Smith and Pridmore, 1989).*

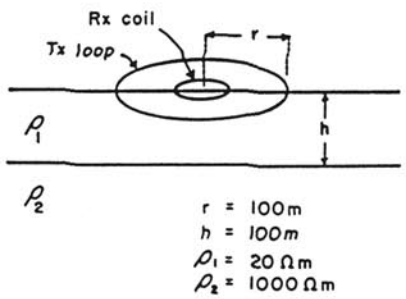

Fig. 2a Typical survey configuration (in-loop).

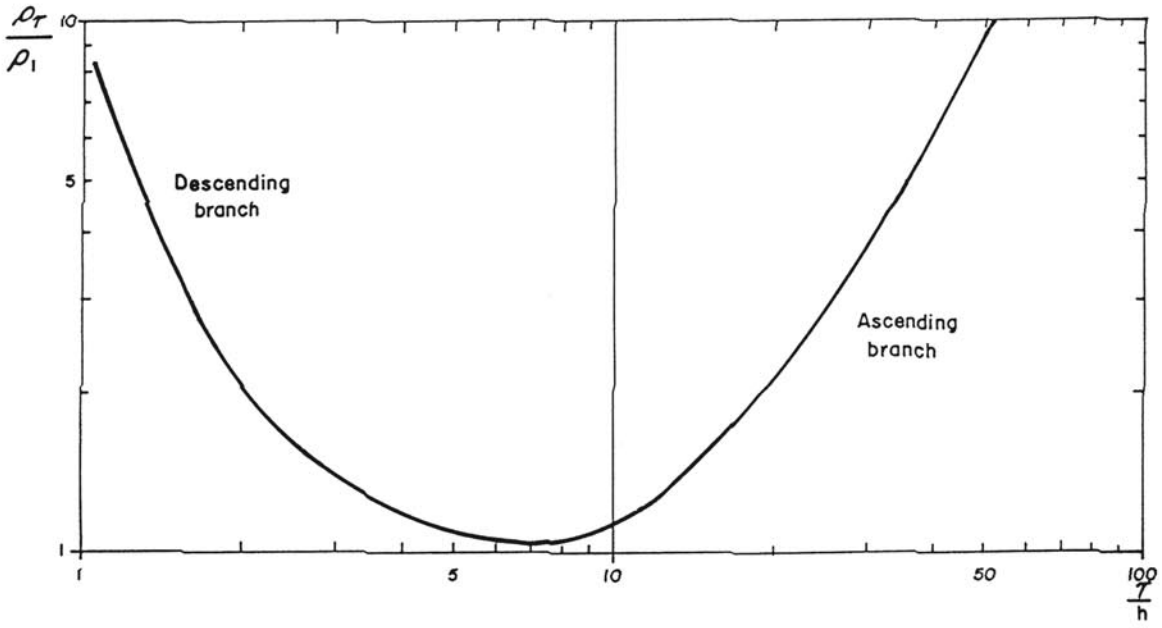

Fig. 2c Dependence of ρ_T/ρ_1 on T/h

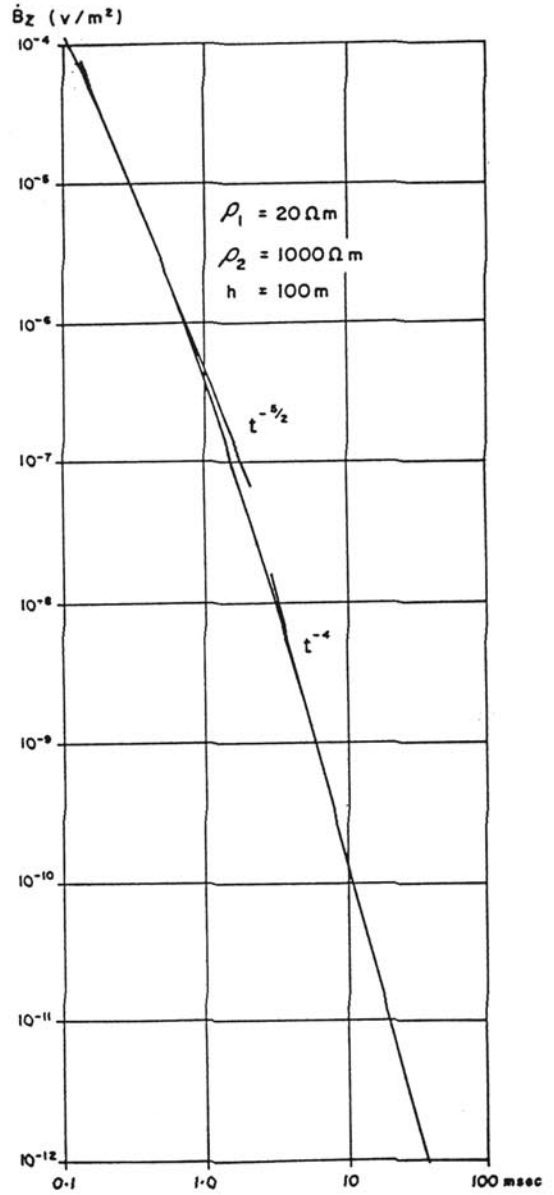

Fig. 2b Time dependence of receiver voltage over a thick conductive overburden overlying resistive bedrock

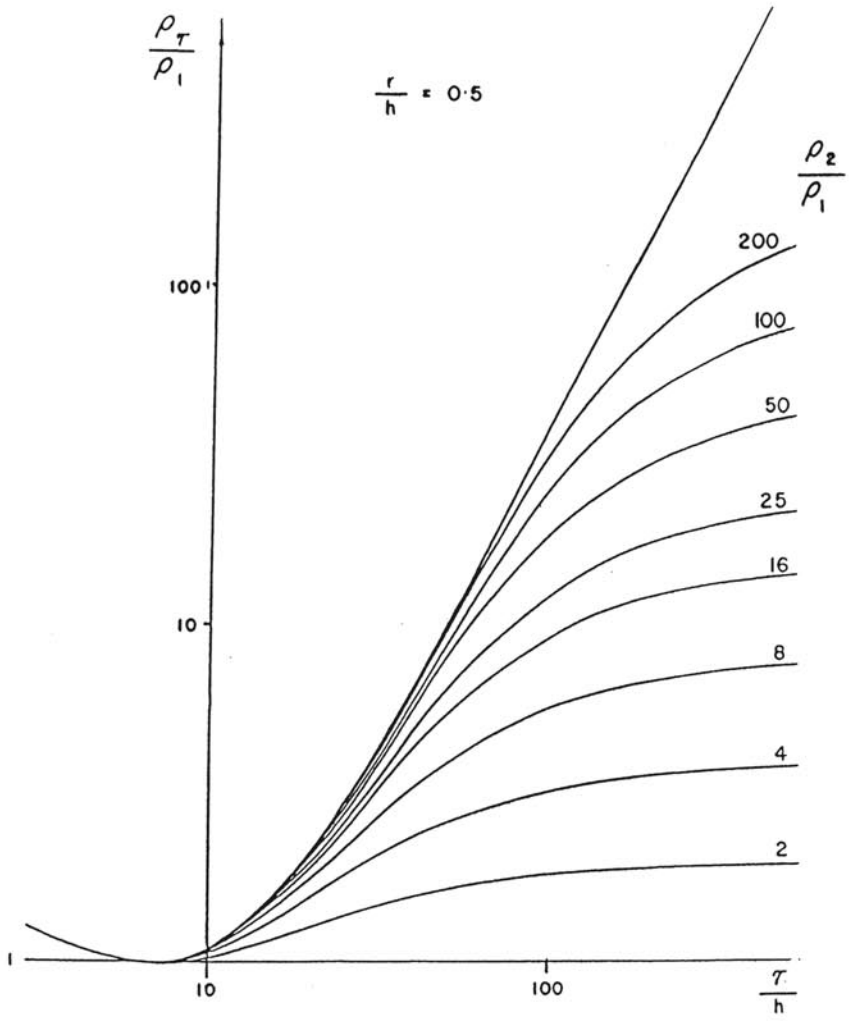

Fig. 2d Dependence of ρ_T/ρ_1 on ρ_2/ρ_1 , r/h = 0.5

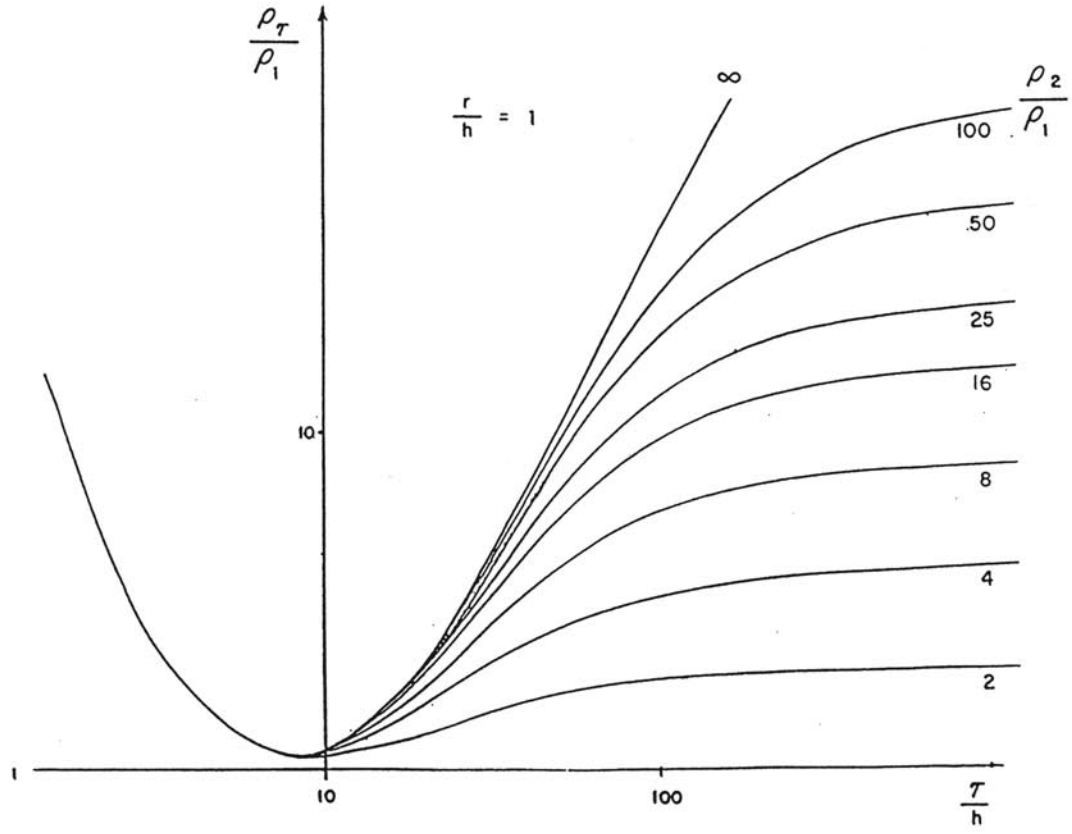

Fig. 2e Dependence of ρ_T/ρ_1 on ρ_2/ρ_1 , r/h = 1.0

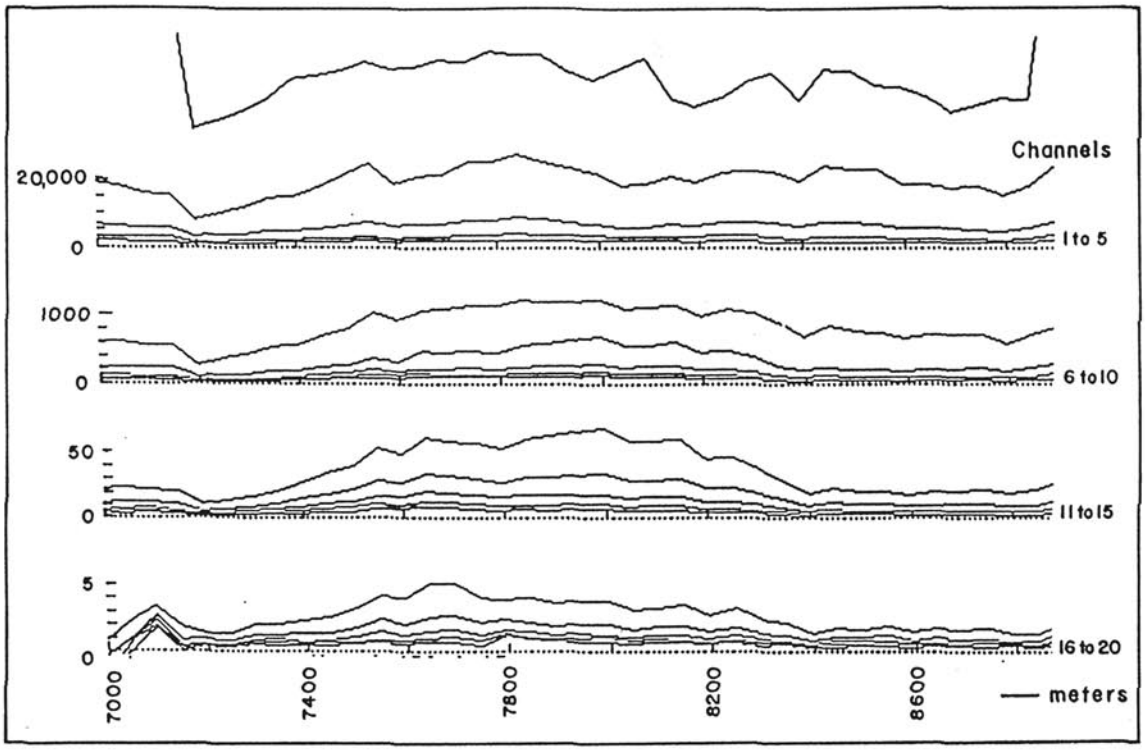

Fig. 3 Profiles (plotted linearly) of Sirotem data, coincident loops 200 x 200m.

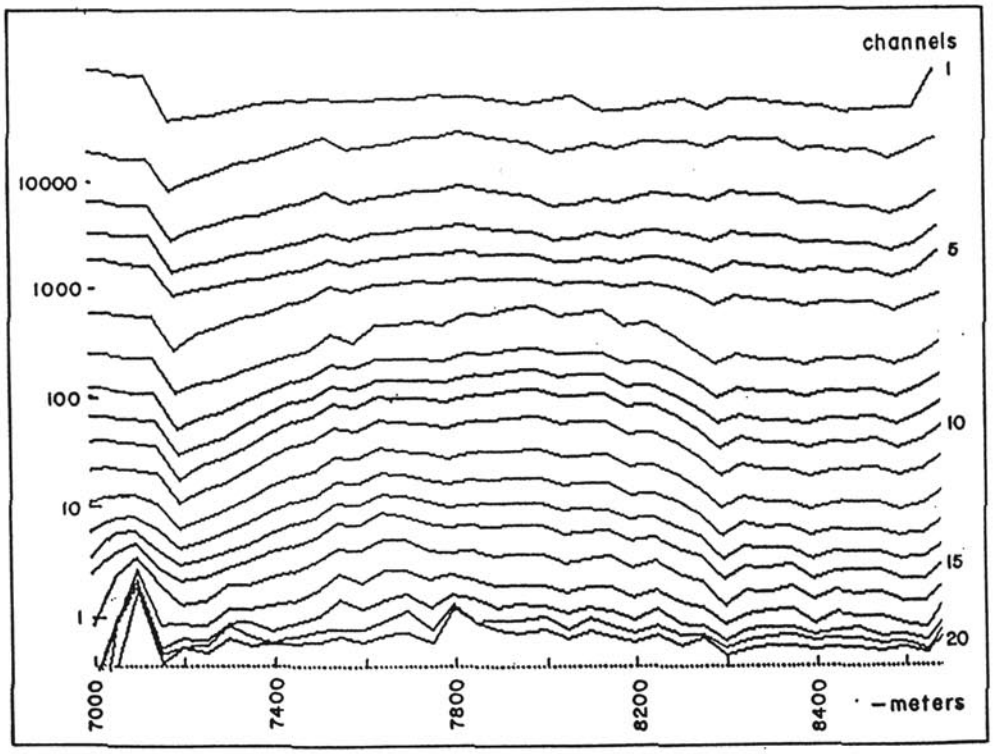

Fig. 4 Data of Fig. 3 plotted logarithmically.

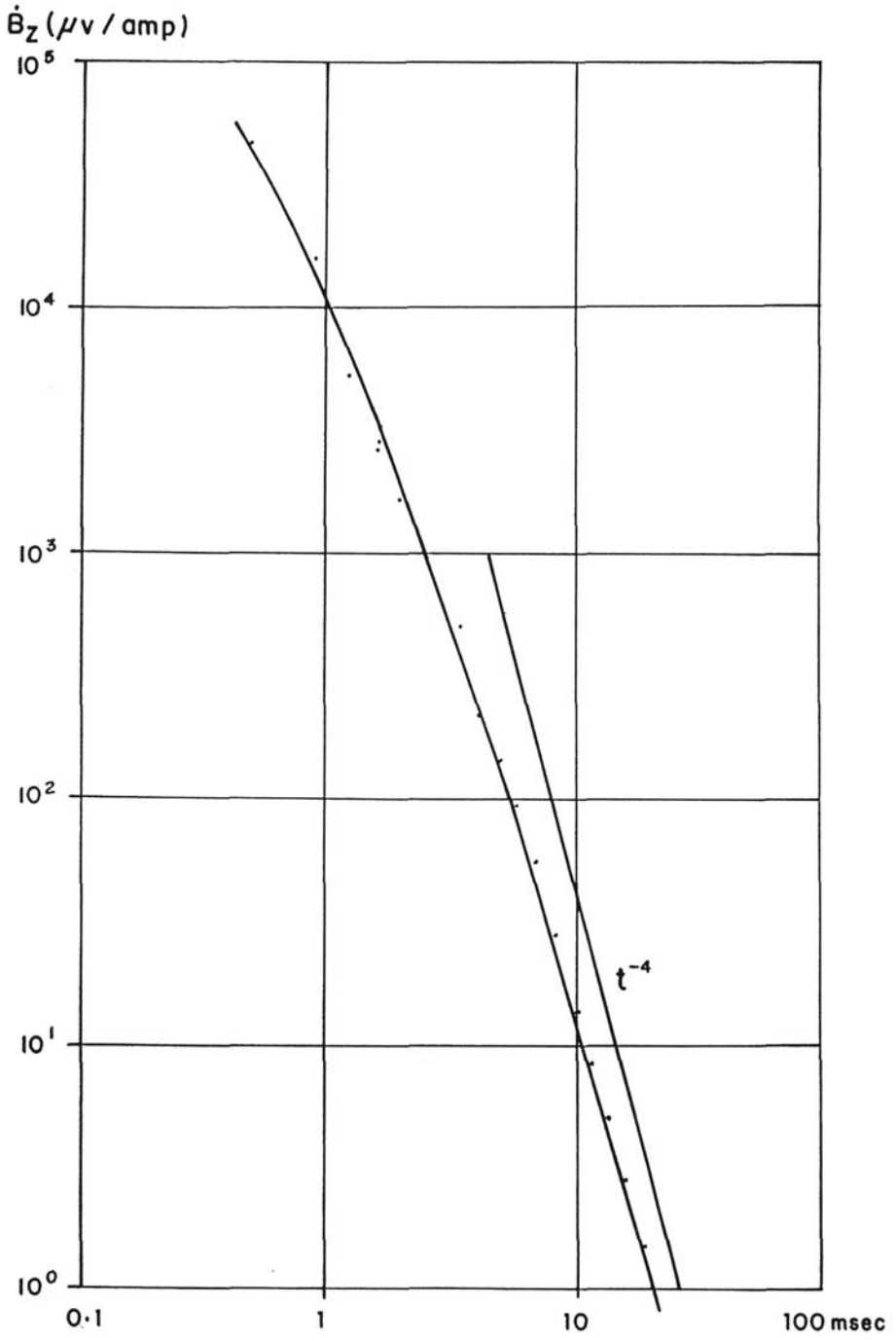

Fig. 5

Transient response at station 8050 of profile in Fig. 3.

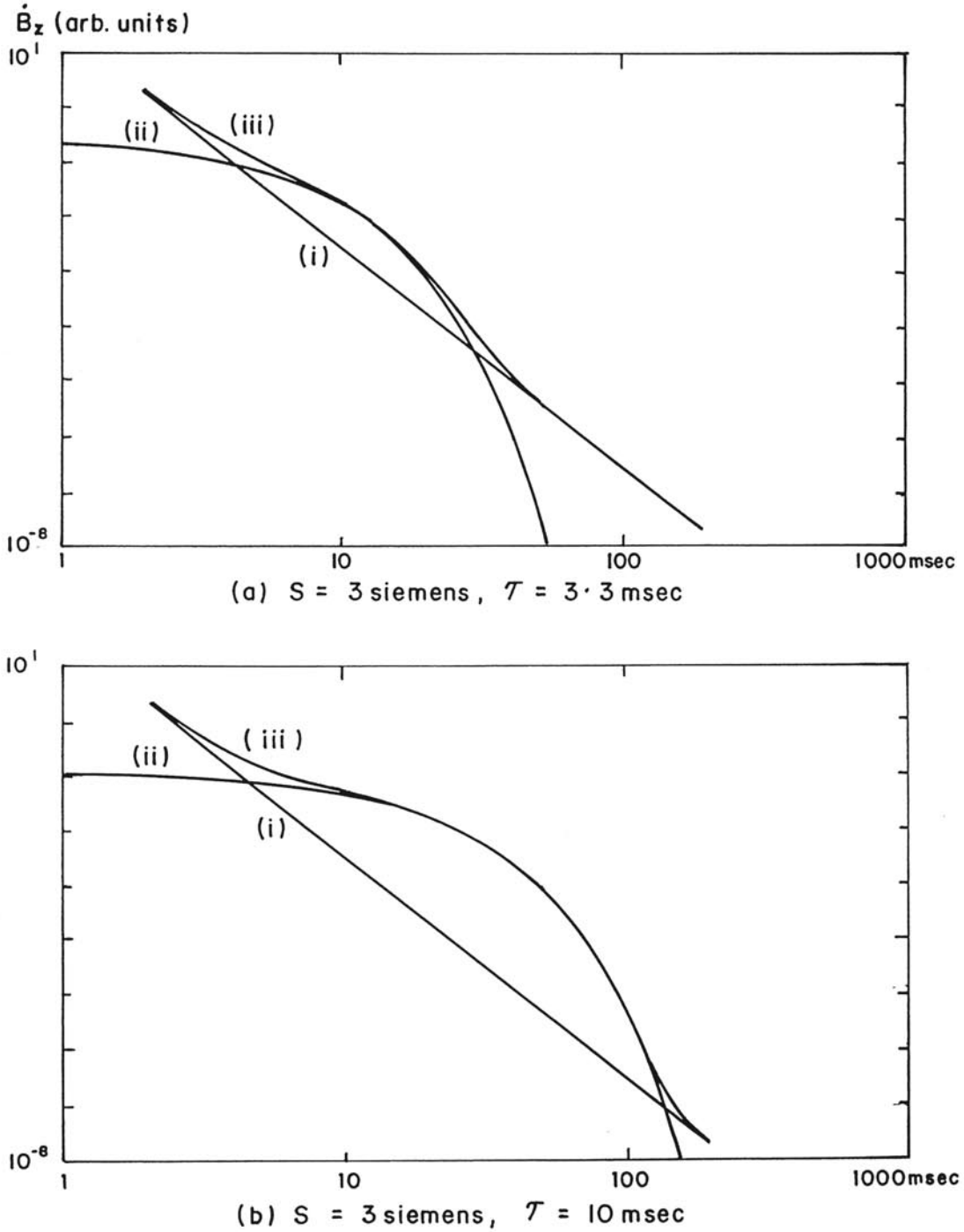

Fig. 6 Decay plots for (i) horizontal thin sheet (ii) exponential decay, and (iii) total response

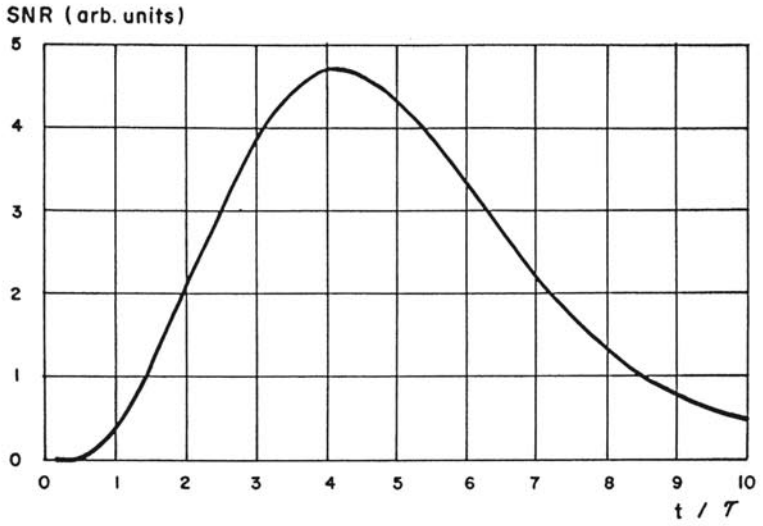

Fig. 7 Plot of signal to noise ratio as a function of t/τ

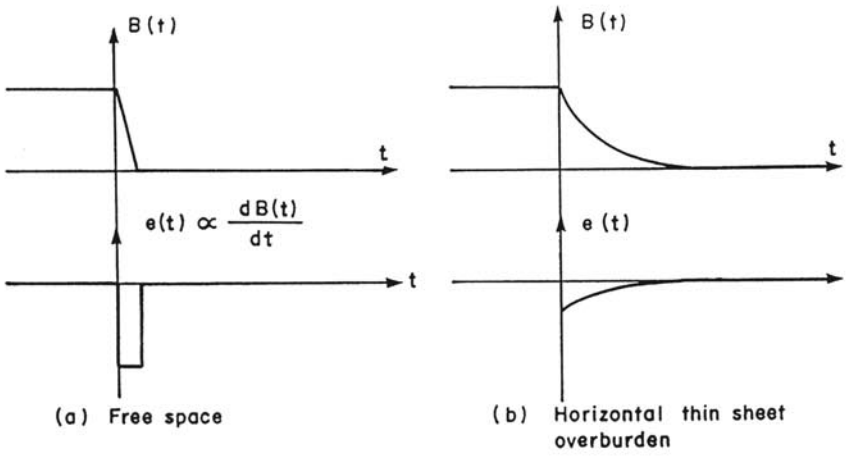

Fig. 8 Distortion of target "drive emf" by conductive overburden

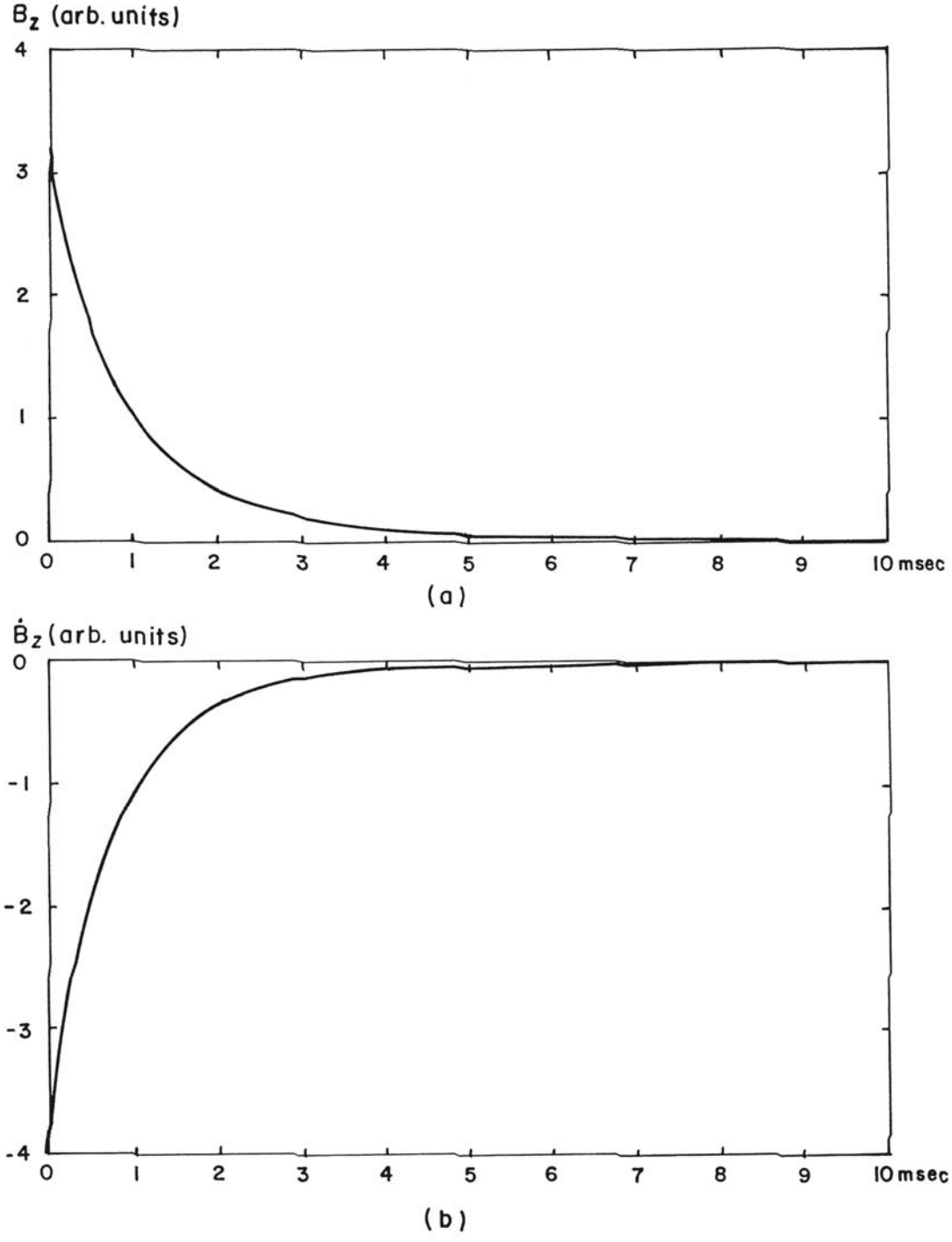

Fig. 9 Time dependence of (a) B_z and (b) $\dot{B}_z$ beneath a 10 siemen horizontal thin sheet.

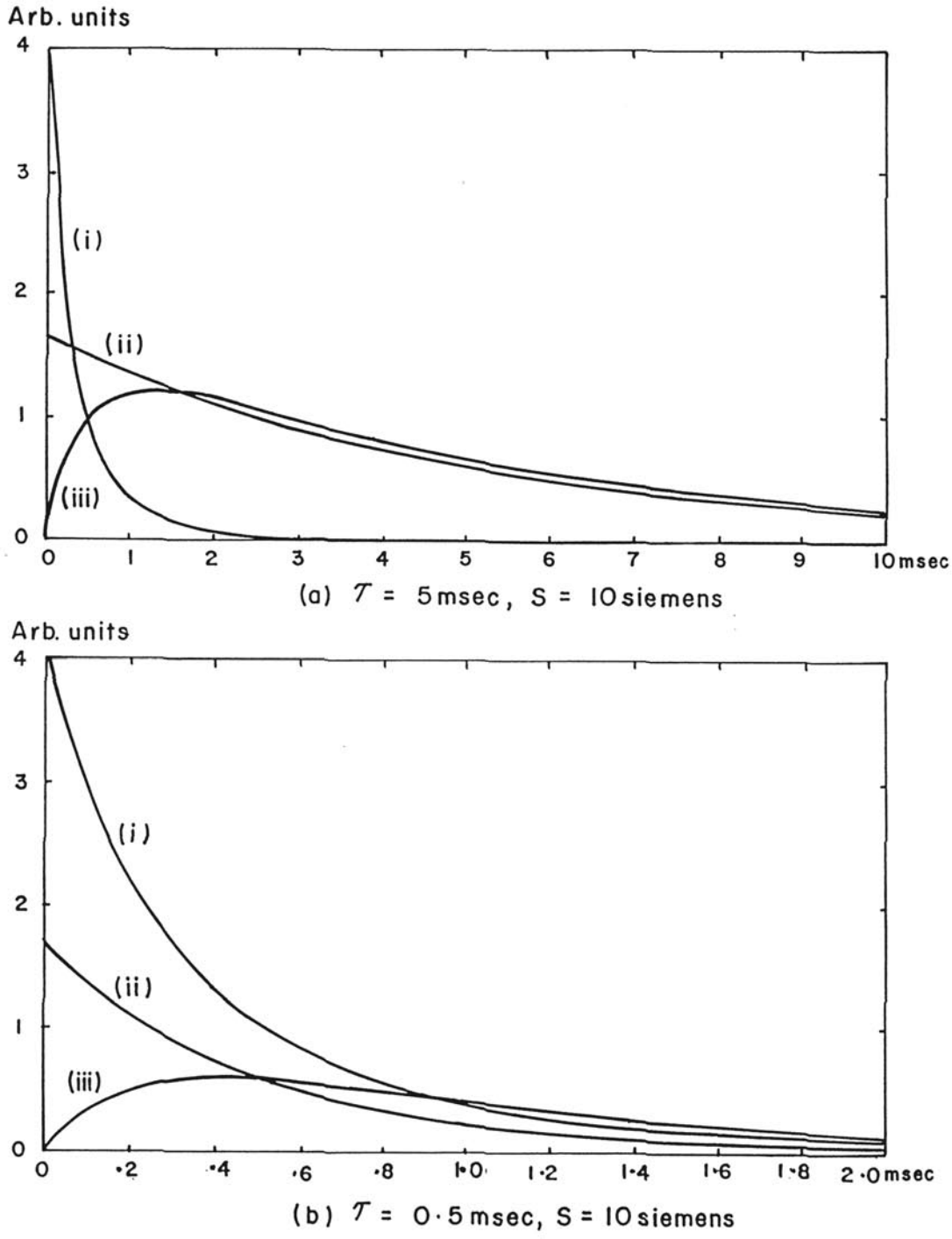

Fig. 10 Time dependence of (i) drive emf, (ii) exponential decay, and (iii) convolution of (i) with (ii).

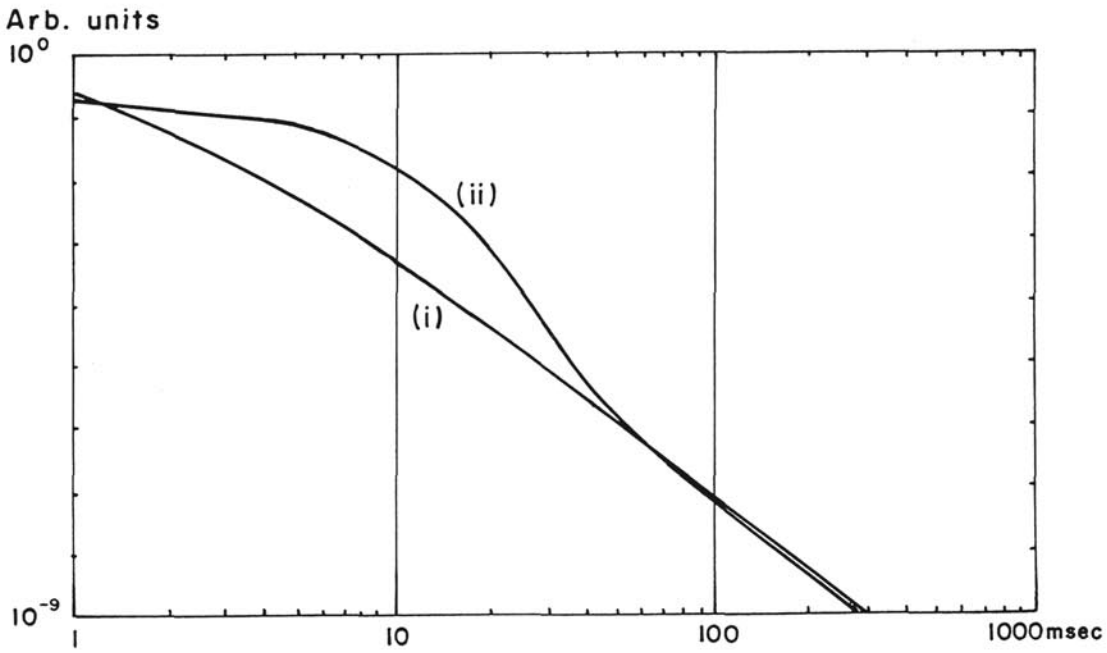

Fig. 10c Time dependence of (i) drive emf and (ii) drive emf convolved with exponential decay, τ = 3msec.

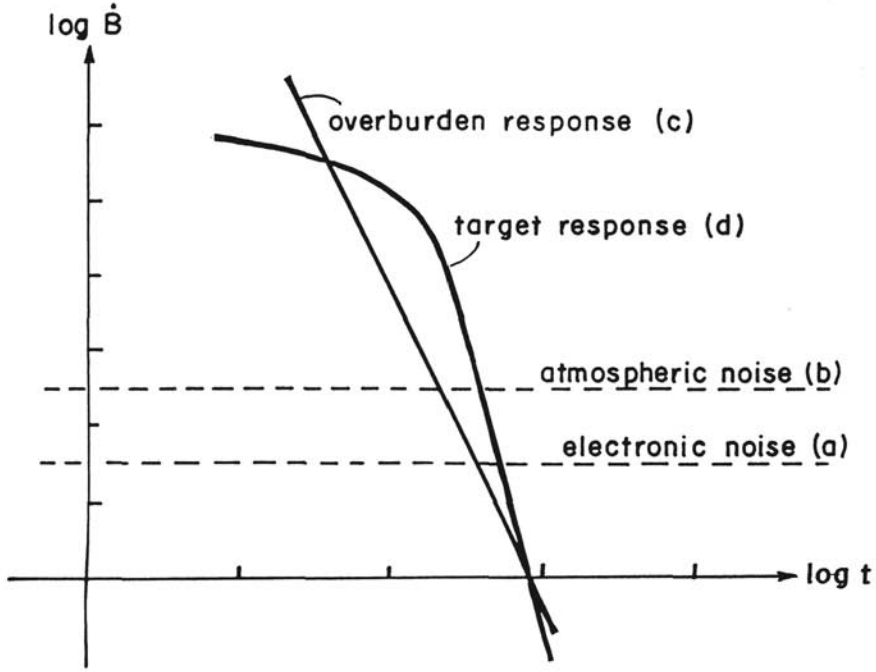

Fig. 11 Sources of noise

Increasing Rx dipole moment simultaneously increases (b), (c) and (d) with respect to (a) so target response is not lost in receiver noise.

Increasing Tx dipole moment simultaneously increases (c) and (d) with respect to (a) and (b) so target response is not lost in atmospheric noise.

For targets of moderate depth reducing the area of Tx and Rx coils (using high current and multi-turns to maintain moments) increases target response with respect to overburden response.

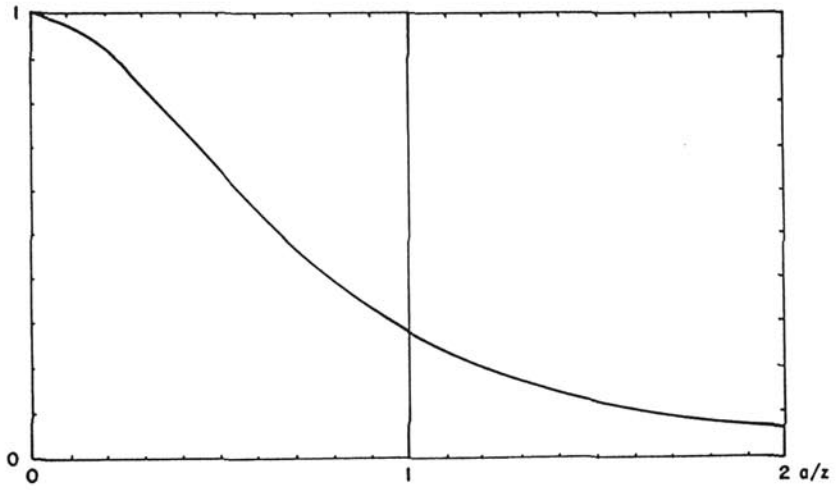

Fig. 12 Relative excitation of a small target to overburden as a function of a/z

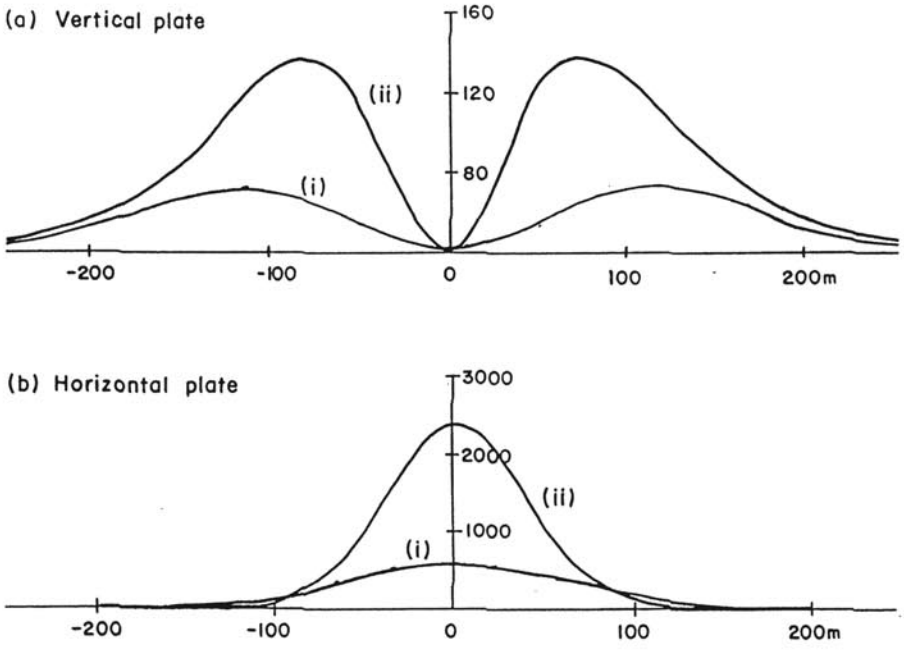

Fig. 13 Calculated profiles over vertical and horizontal plates (i) both transmitter and receiver 200 x 200m loops and (ii) transmitter 100 x 100m, dipole receiver.

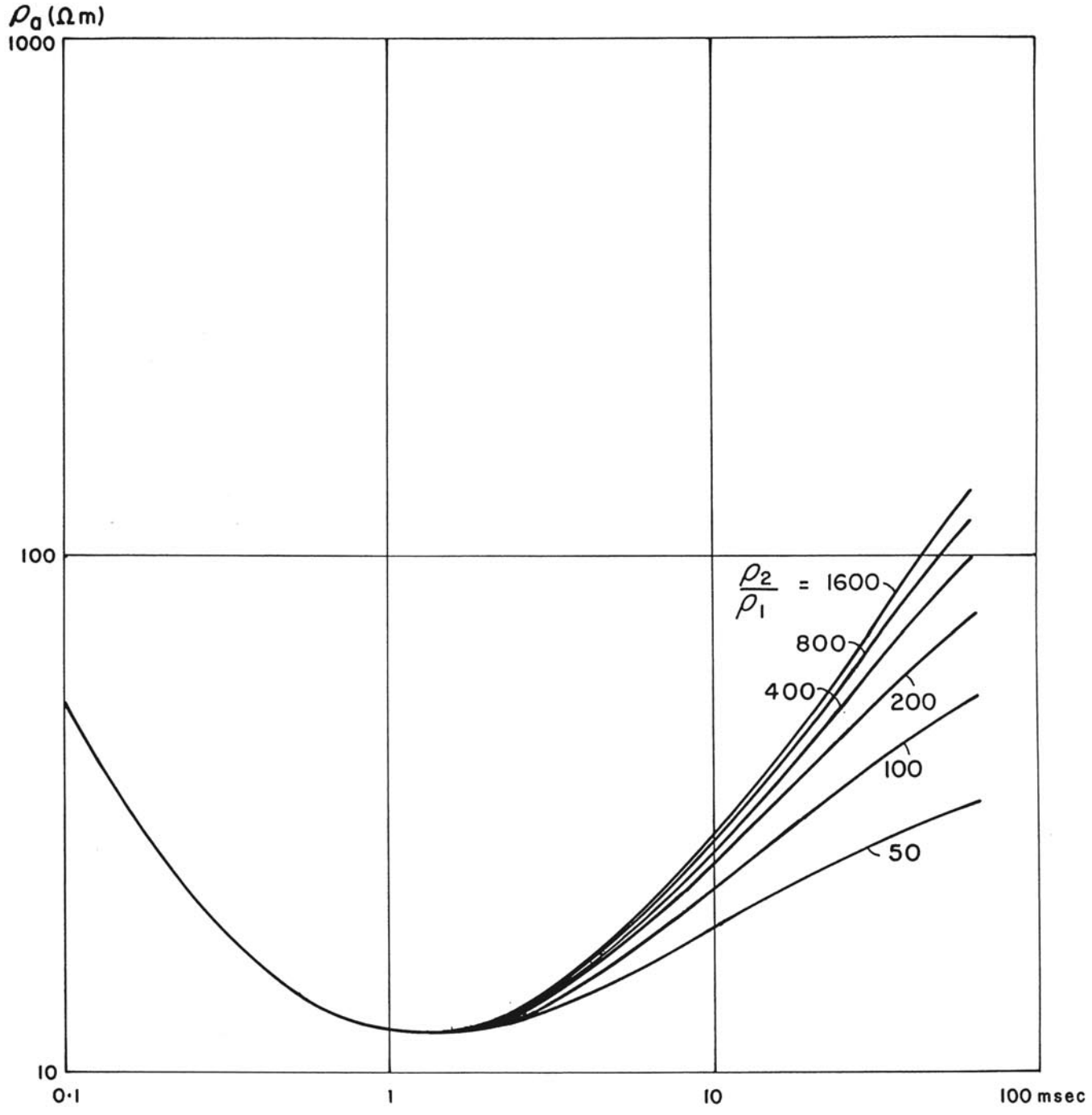

Fig. 14 Apparent resistivity of thick overburden response as a function of ρ_2/ρ_1

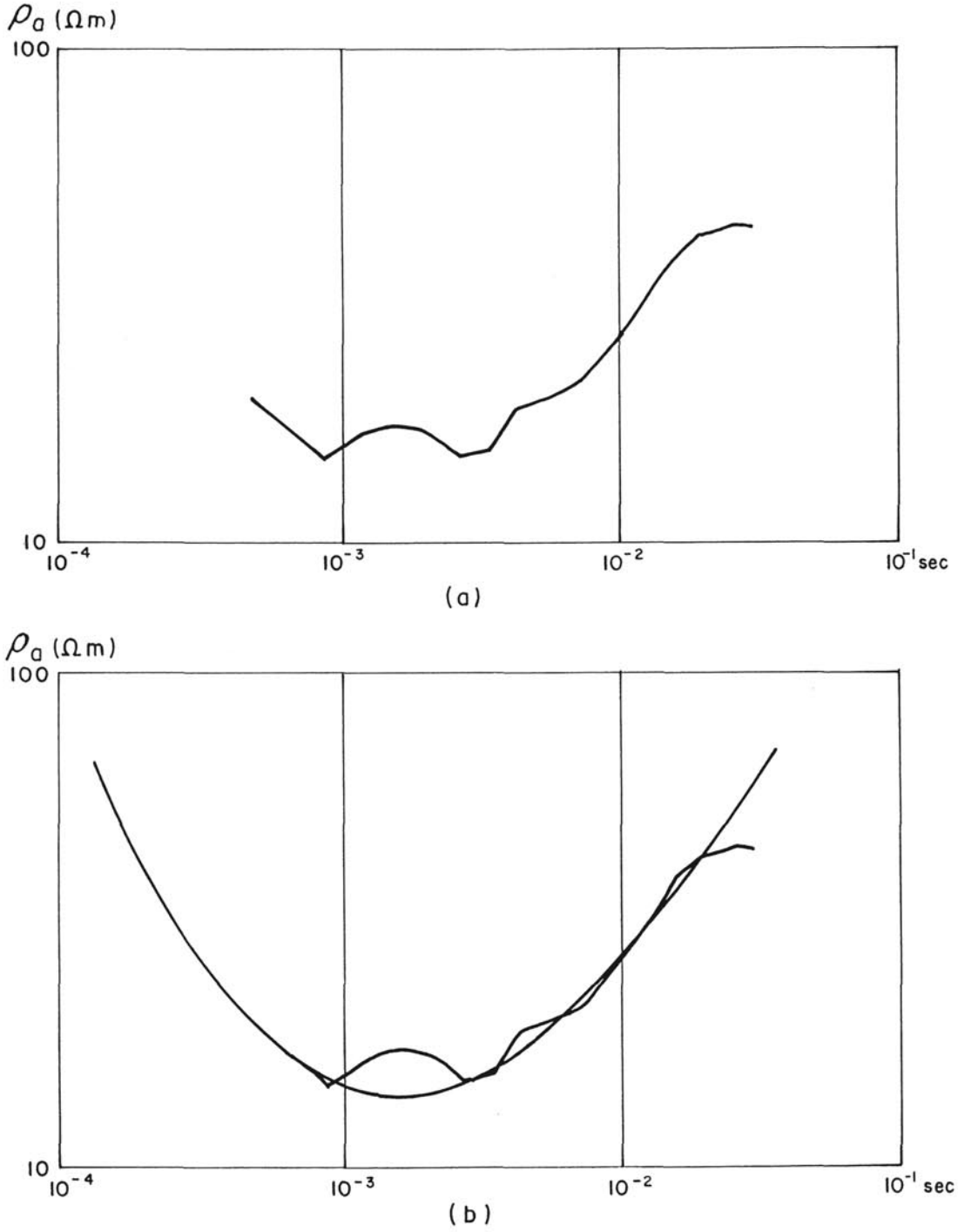

Fig. 15 Data of Fig. 5, (a) replotted as apparent resistivity and (b) superimposed on a two layer curve of the type shown in Fig. 14.

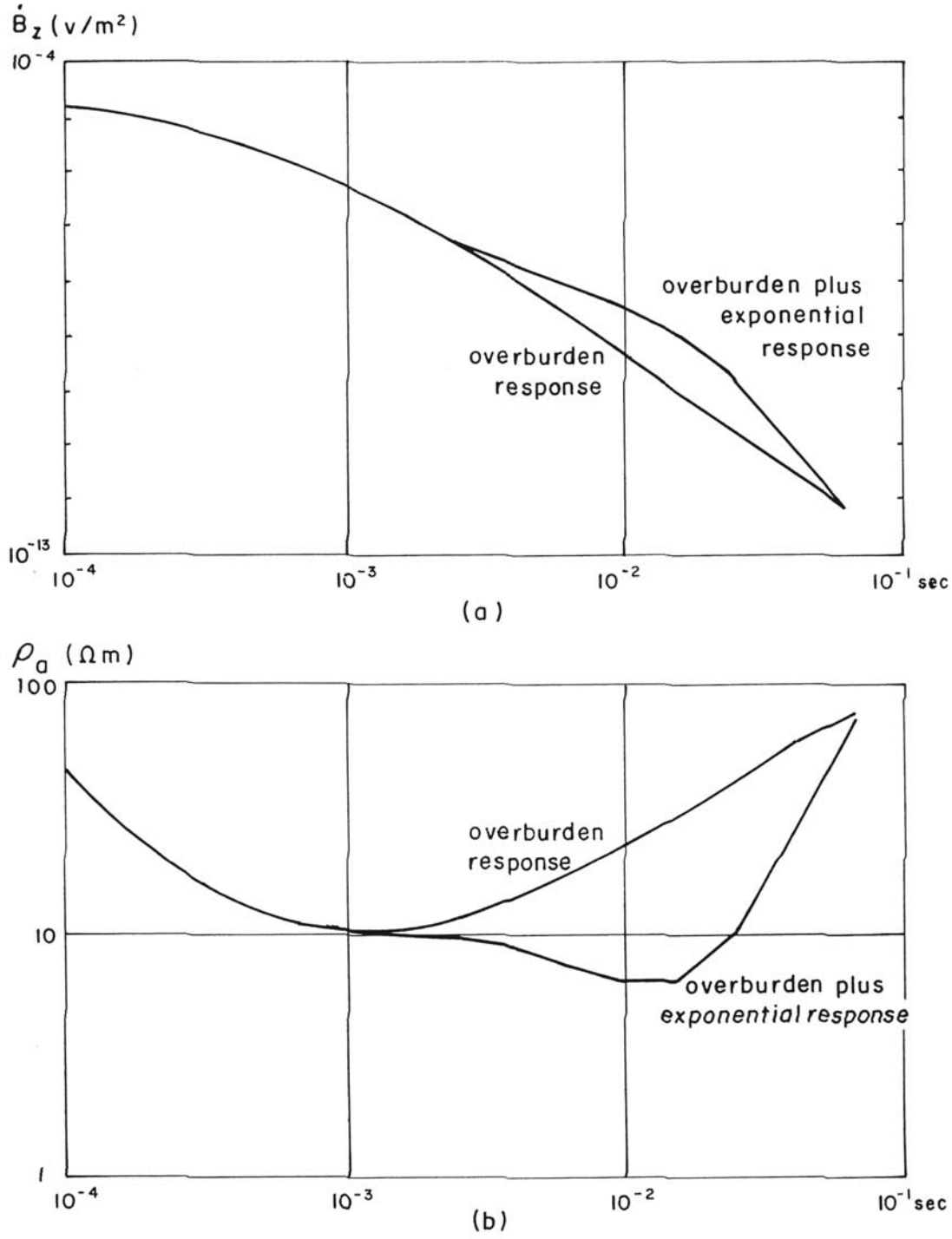

Fig. 16 Effect of adding an exponential anomaly to typical *overburden response*

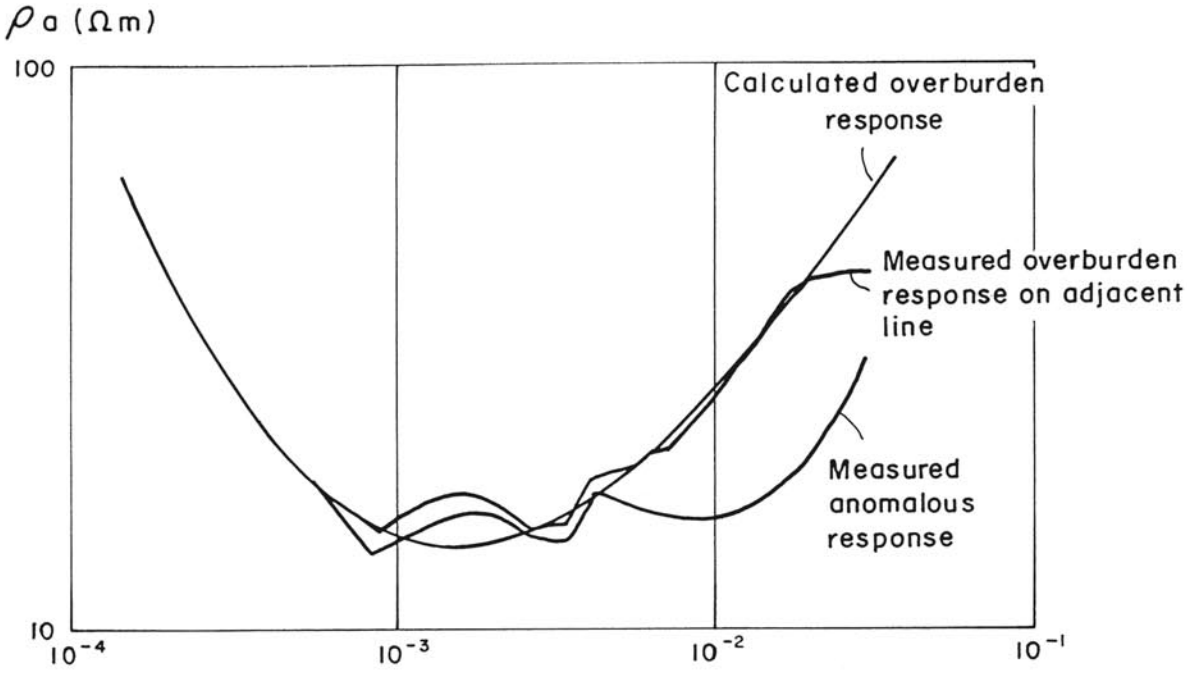

Fig. 17

Anomaly-free and anomalous responses plotted as apparent resistivity.